

Supplementary Table S1: Patients' characteristics

Nb. of patients	type	Nanostring			Immunohistochemistry			
		nRT	nCRT	p value	No nCRT	nRT	nCRT	p value
		n. (%)	n. (%)		n. (%)	n. (%)	n. (%)	
		13	30		12	8	13	
Age	Over 65y	6 (46.2%)	13 (43.3%)	1	7 (58.3%)	3 (37.5%)	4 (30.8%)	0.9
	Under 65y	7 (53.8%)	17 (56.7%)		5 (41.7%)	5 (62.5%)	9 (69.2%)	
Gender	Female	4 (30.8%)	7 (23.3%)	0.7	5 (41.7%)	2 (25%)	3 (23.1%)	0.6
	Male	9 (69.2%)	23 (76.7%)		7 (58.3%)	6 (75%)	10 (76.9%)	
Cancer location	Colon	-	-	0.4	4 [#] (33.3%)	-	-	0.03
	Inf. Rectum	8 (61.5%)	16 (53.3%)		4 (33.3%)	6 (75%)	6 (46.2%)	
	Mid. Rectum	2 (15.4%)	10 (33.3%)		2 (16.7%)	2 (25%)	7 (53.8%)	
	Sup. Rectum	3 (23.1%)	4 (13.3%)		2 (16.7%)	-	-	
RT duration	Long Course	7 (53.8%)	30 (100%)	0.0004	-	8 (100%)	13 (100%)	1
	Short Course	6 (46.2%)	0		-	-	-	
cTNM	II	1 (7.7%)	7 (23.3%)	0.1	-	-	-	1*
	III	9 (69.2%)	22 (73.3%)		-	8 (100%)	13 (100%)	
	IV	3 (23.1%)	1 (3.3%)		-	-	-	
pTNM	0	1 (7.7%)	NA (NA%)	0.1	-	1 (12.5%)	-	0.4
	I	2 (15.4%)	7 (23.3%)		1 (8.3%)	1 (12.5%)	-	
	II	2 (15.4%)	13 (43.3%)		3 (25%)	3 (37.5%)	7 (53.8%)	
	III	5 (38.5%)	8 (26.7%)		5 (41.7%)	3 (37.5%)	5 (38.5%)	
	IV	3 (23.1%)	2 (6.7%)		3 (25%)	-	1 (7.7%)	
Center[§]	Belgium	6 (46.2%)	16 (53.3%)	0.7	-	-	-	1
	Roumania	7 (53.8%)	14 (46.7%)		12 (100%)	8 (100%)	13 (100%)	

*p= 0.03 if cTNM of neoadjuvant patients is compared to pTNM of surgically-treated patients

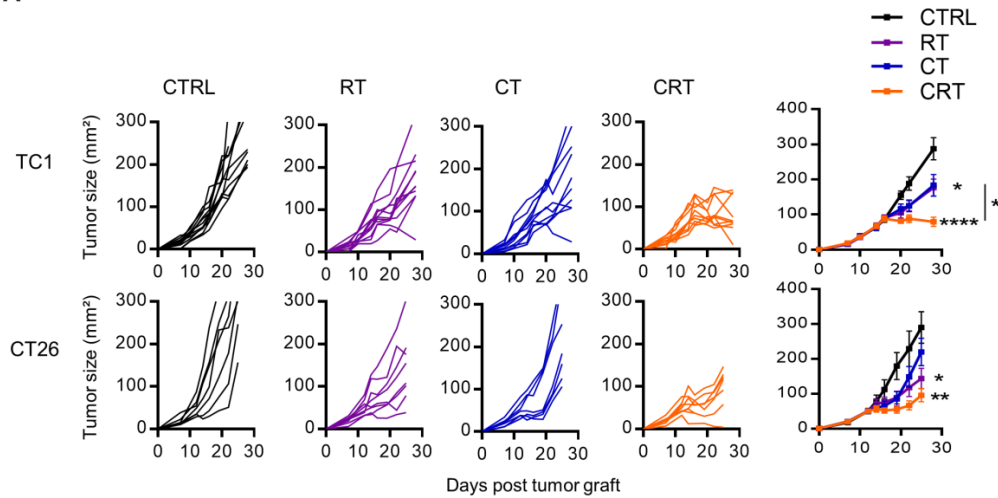
3 sigmoid colon and 1 Splenic flexure

§ Belgium= Institut Roi Albert II, Brussels, Belgium; Roumania=Regional Institute of Oncology, Iasi, Roumania

nRT= neoadjuvant radiotherapy, nCRT = neoadjuvant chemoradiotherapy

Supplementary Figure S1 related to Fig.2

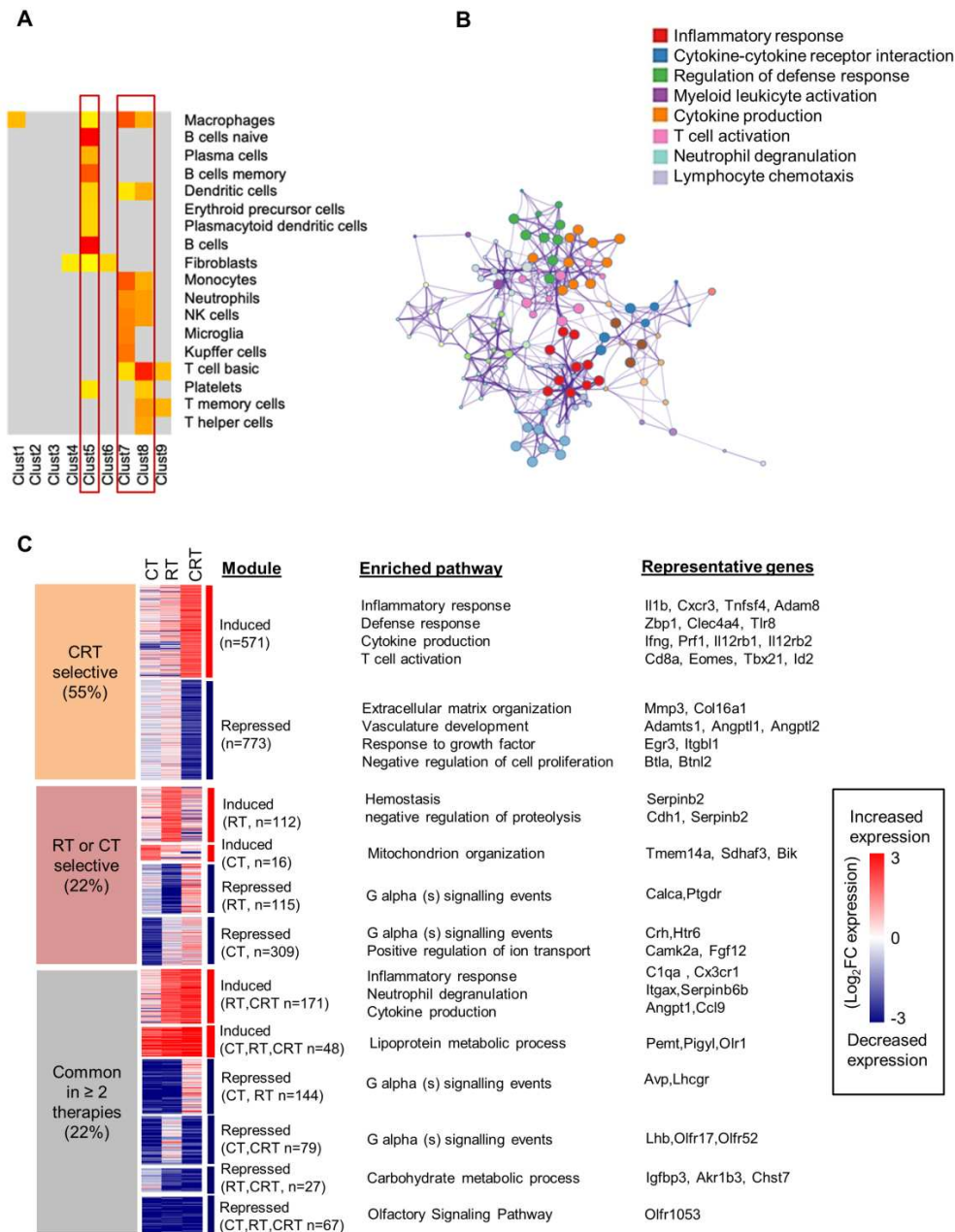
A



Supplementary Figure S1

(A) C57BL/6N and BALB/cAnCr mice were injected subcutaneously with 2×10^5 TC1-HPV16⁺ and CT26 colon tumor cells, respectively. Mice were treated with chemotherapy (CT), radiotherapy (RT), or chemoradiotherapy (CRT) when the tumors reached 50-60 mm² (n = 10 mice/treatment group, 3 experiments). Tumor growth of treated mice is shown.

Supplementary Figure S2 related to Fig.2 and 3

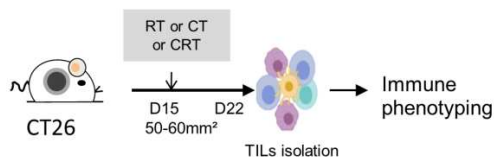


Supplementary Figure S2

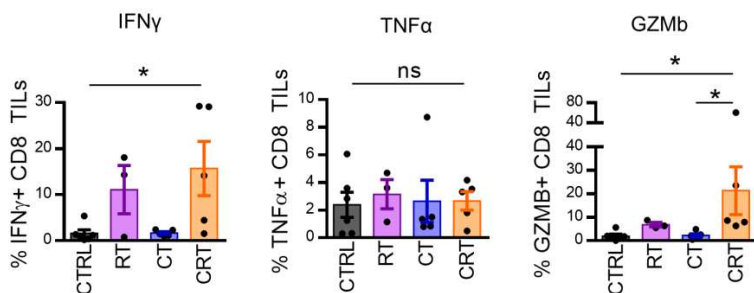
(A) Heatmap showing \log_{10} normalized Fragments Per Kilobase of transcript per Million mapped reads (FPKM) of DEGs related to T-cell expressed in TILs from CTRL, RT, CT, and CRT-treated TC1-bearing mice (n = 6 mice/treatment group). Gene set enrichment analysis was performed using the PanglaoDB gene specific genes sets. Twenty-seven gene sets with more than 10 genes in a cluster and presenting a corrected p-value below 0.01 were selected. (B) Network of pathways selectively induced in tumor-infiltrating immune cells from the CRT-treated mice. Data are representative of TC1 tumor model. (C) Genes and pathways regulated in TILs from CT, RT and CRT-treated mice bearing TC1 tumors. Key pathways enriched in each group of DEGs are indicated as well as representative DEGs from each pathway. Heatmap displays \log_2 FC in expression, Treatment versus untreated control. (n=1 for each condition and represents a pool of TILs from at least 6 mice). CTRL=untreated mice, RT: radiotherapy, CT: chemotherapy and CRT: chemoradiation. See also Figure 2.

Supplementary Figure S3 related to Fig.3

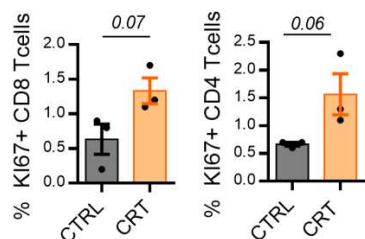
A



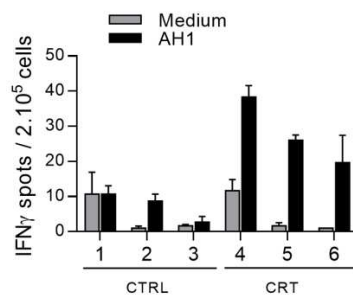
B



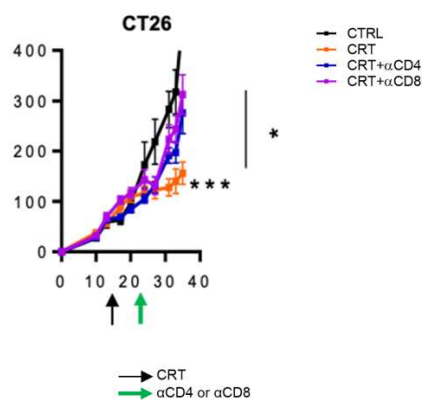
C



D



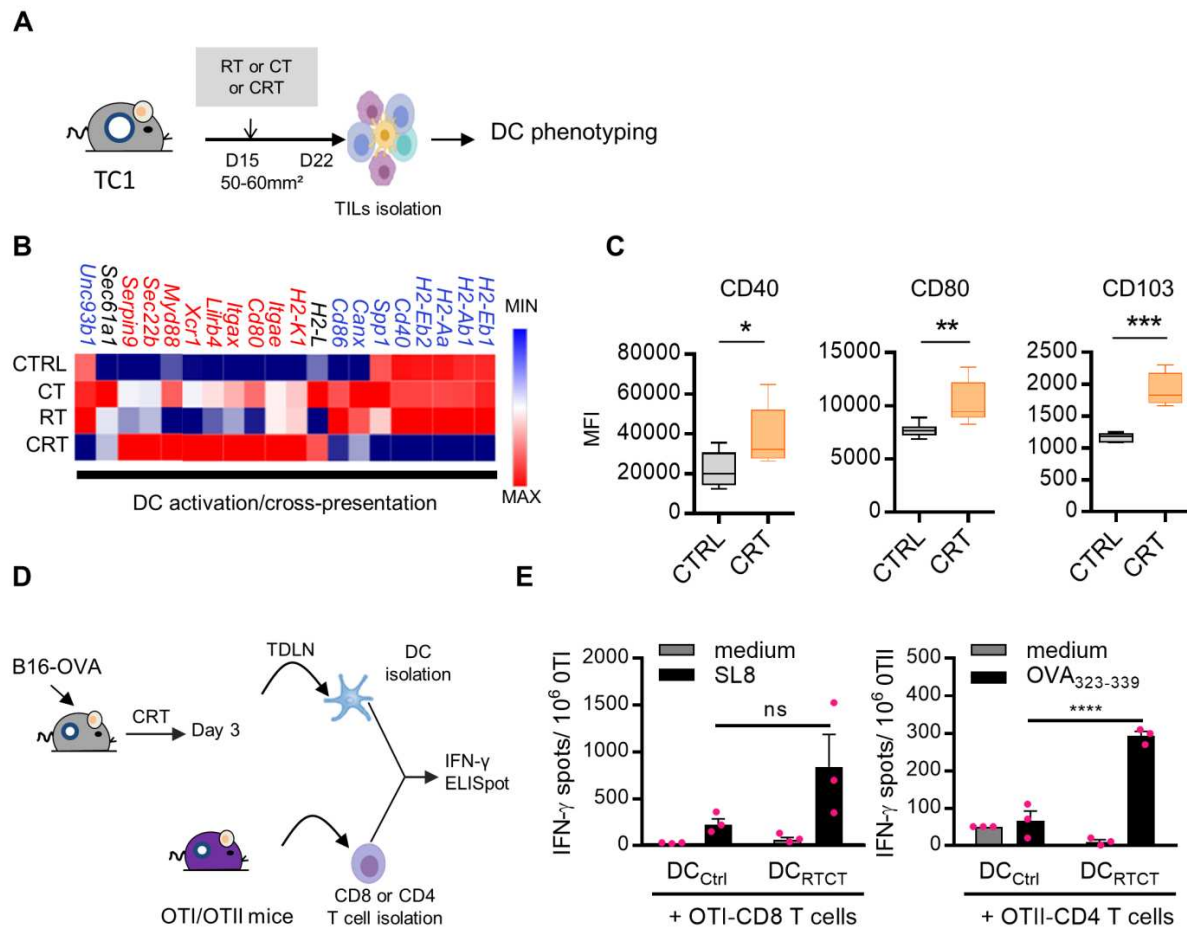
E



Supplementary Figure S3

(A) Experimental design. (B) Scatter plots comparing percentage of IFN- γ , TNF α , and granzyme B (GZMB) production assessed by intracellular cytokine staining after 6 hours of stimulation with AH1-derived class I peptide in CT26 tumor model. (C) Scatter plots showing percentages of Ki67-expressing CD8+ (left) and CD4+ (right) TILs in untreated and CRT-treated CT26-bearing mice (Means \pm SEM). (D) Functional analysis of CD8 T cells splenocytes measured by the IFN- γ ELISpot assay after 20 hours of stimulation with AH1-derived peptide. (E) Tumor growth of CT26 mice receiving three injections of anti-CD4⁺ or CD8⁺ antibodies 7 days post-CRT. The one-way ANOVA and Kruskal-Wallis tests were used; * p < 0.05, *** p < 0.001.

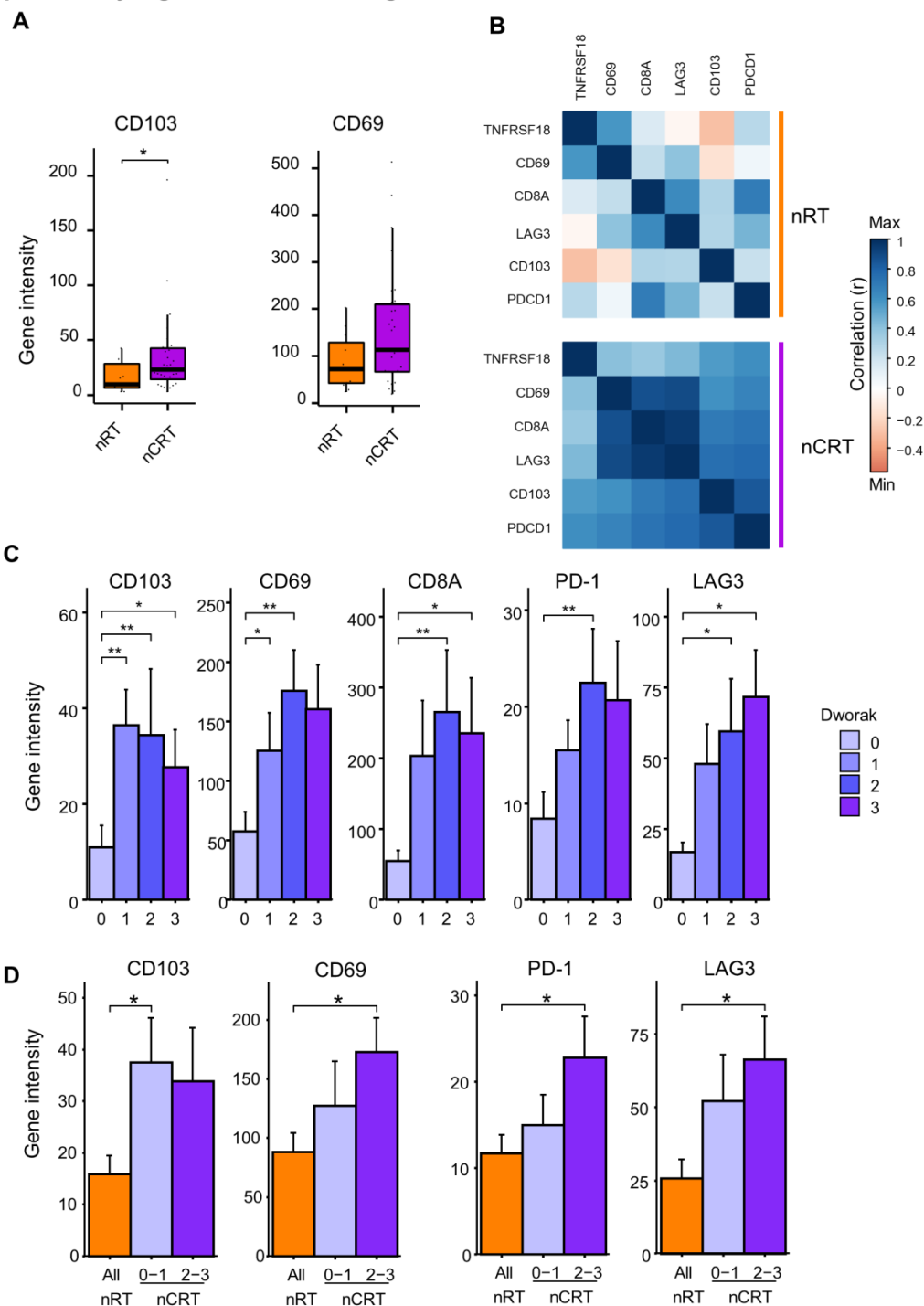
Supplementary Figure S4 related to Figure 3



Supplementary Figure S4.

(A) Experimental design. **(B)** Heatmap showing the log₂ normalized FPKM of DEGs related to dendritic cell activation and cross-presentation expressed in TILs in the CTRL, RT, CT, and CRT-treated mice (n = 6 mice/ treatment group). **(C)** Mean fluorescence intensity (MFI) of CD80+, CD40+, and CD103+ on CD11c⁺ dendritic cells isolated from the CTRL and CRT-treated mice tumor-draining lymph nodes (TDLN) 3 days post-therapy (Data are representative of two experiments and are expressed as means ± SEM; n = 3-6 mice/treatment group). **(D)** Dendritic cells from TDLN of CRT-treated B16-OVA tumor-bearing mice were magnetically sorted and cocultured with OTI or OTII T cells. **(E)** Functional analysis of OTI and OTII T cells measured by IFN-γ ELISpot assay after coculture with sorted dendritic cells (Data are representative of one experiment out of two; n = 3 mice/treatment group). The Mann-Whitney and Kruskal-Wallis tests were used; *p < 0.05, **p < 0.01, ***p < 0.001.

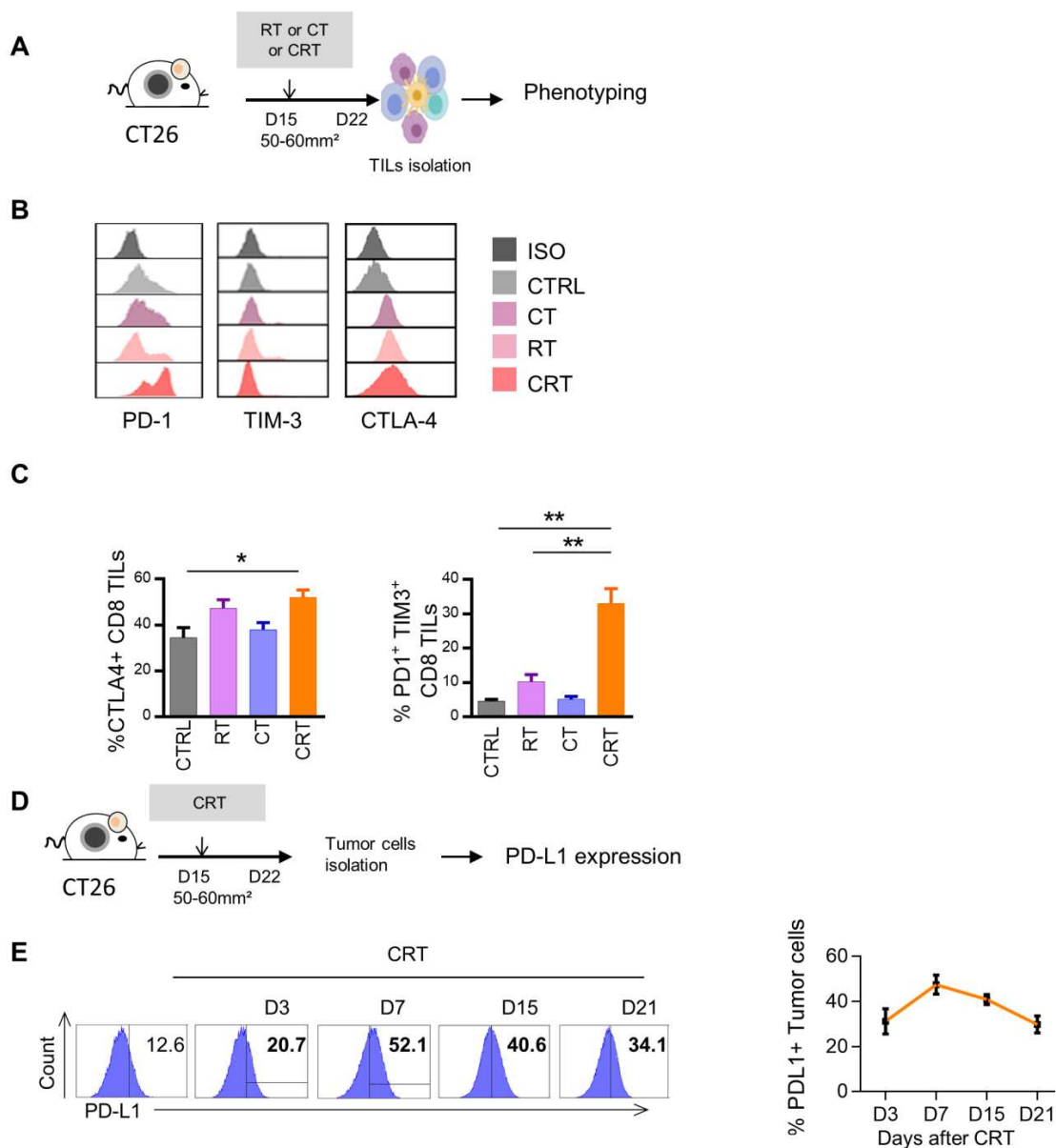
Supplementary Figure S5 related to Figures 1 and 4



Supplementary Figure S5:

(A) Expression level of T_{RM} associated genes in nRT or nCRT treated tumors. **(B)** Correlation matrix of T_{RM} associated genes in nRT (top) or nCRT (bottom) treated tumors. **(C)** Expression level of T_{RM} associated genes in tumors with increasing histologic response to neoadjuvant treatment (Dworak 0, 1, 2 and 3). **(D)** Expression level of T_{RM} associated genes in tumors treated with nRT and with increasing histologic response to nCRT (Dworak 0-1 and 2-3). nRT=neoadjuvant radiotherapy, nCRT=neoadjuvant chemoradiotherapy. P^* = Unilateral linear-by-linear association test.

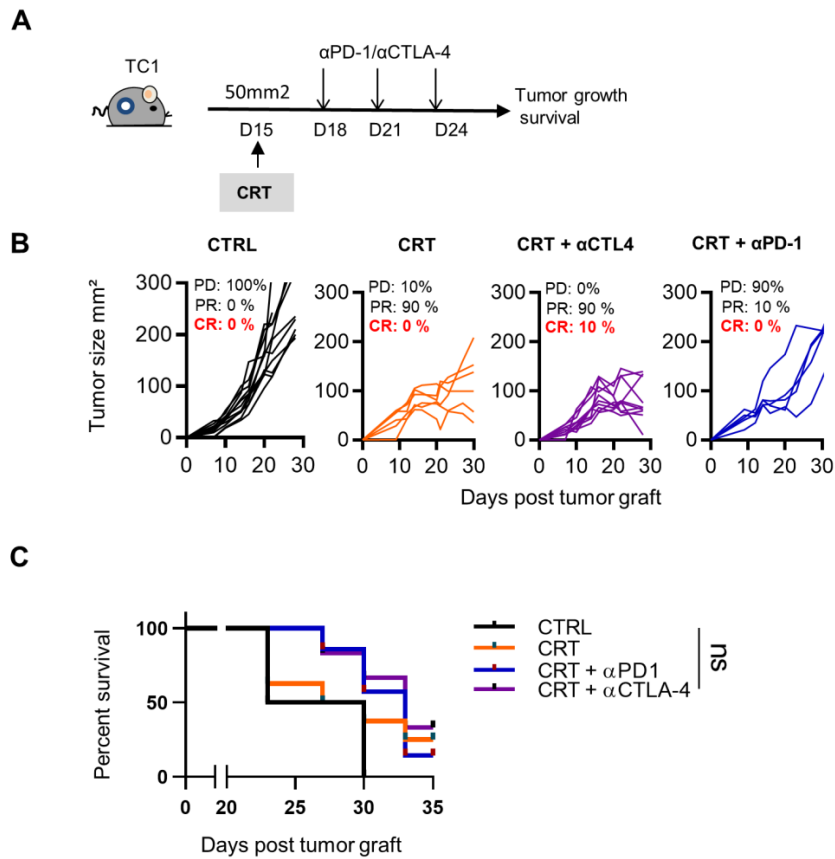
Supplementary Figure S6 related to Figure 5



Supplementary Figure S6.

(A) BALB/cAnCrI mice were injected subcutaneously with 2.10^5 CT26 colon tumor cells, respectively. Mice were treated with chemotherapy (CT), radiotherapy (RT), or chemoradiotherapy (CRT) when the tumors reached 50-60 mm² (n = 10 mice/treatment group, 3 experiments) (B) Flow cytometry histograms of PD1, TIM3 and CTLA-4 expression on CD8⁺ TILs in CTRL, RT, CT, and CRT-treated mice 7 days post-treatment. (C) Histograms showing percentages of CTLA-4 expression (left) and PD-1+TIM-3 co-expression (right) on total CD8⁺ TILs. (Data expressed as means \pm SEM). (D) Experimental design. (E) Flow cytometry dot plot graphs of PD-L1 expression (left) and percentages associated (right) in CT26 model.

Supplementary Figure S7 related to Figure 6



Supplementary Figure S7.

(A) TC1 tumor-bearing mice received or not a single injection of anti-CTLA-4 (200 μ g ip) 2 days before CRT followed by three injections of anti-PD-1 or CTLA-4 antibodies (200 μ g ip each) 3 days post-CRT. Experimental scheme is depicted. **(B)** Tumor growth of CTRL, and CRT-treated mice with or without anti-CTLA-4 or PD-1 therapy. Tumor responses (progressive disease [PD], partial response [PR], complete response [CR]) are indicated. **(C)** Survival curves associated. The Bonferroni method was used.

SUPPLEMENTARY METHODS

Patients

Immunohistochemistry and image analysis

Surgical specimens from 34 colorectal cancer patients (nRCT, n = 20) were analyzed by immunohistochemistry. Three formalin-fixed paraffin-embedded (FFPE) tissue sections of 4 microns were processed for immunohistochemistry with anti-PD-1 (NAT105, 2.21 µg/mL; Ventana, Tuscon, AZ, USA), anti-PD-L1 (E1L3N, 10 µg/mL; Cell Signaling, Leiden, The Netherlands), and anti-LAG3 (11E3, Abcam, 0.5 µg/mL) antibodies according to the in-house protocol and were revealed with the Ultra view Universal DAB IHC Detection Kit (Ventana) and counterstained with Mayer's Hematoxylin. Digital slides were imaged with a 20x magnification to a resolution of 0.45 µm/pixel (Nano zoomer XD, Hamamatsu, Japan). A strict delimitation of the tumor component excluding normal tissue and low/high grade dysplasia-associated lesions was confirmed by an expert pathologist. The mean densities of PD-1⁺ and LAG3⁺ cells in the tumor region were determined with the HALO™ image analysis system (Indica Labs, Corrales, NM). PD-L1 expression on tumor cells and TILs was assessed according to the previously described score [1]. Tumor cells were scored as percentage of PD-L1-expressing tumor cells (<1%, >1-5%, >5-50%, >50%) and TILs as percentage of the tumor area (<1%, >1-5%, >5-50%, >50%).

Human RNA extraction and transcriptomic analysis by Nanostring technology

Three 20 microns thick FFPE tissue sections from 43 rectal tumors surgically removed after nCRT and from 13 tumors not treated by nCRT were processed. Total RNA isolated using the RecoverAll™ Total Nucleic Acid Isolation Kit (Ambiom, ThermoFisher, Monza, Italy) was tested for its quality and quantity with the Agilent RNA 6000 Nano kit (Agilent Technologies, Santa Clara, CA) and NanoDrop 2000 (ThermoFisher Scientific, Waltham, USA). 100-400 ng of RNA extracted from each tumor was tested (Nanostring Technologies, Seattle, WA, USA) with an in-house panel of 44 immune-related genes (see supplementary table S1). Reporter-capture probe pairs were hybridized and the resulting RNA complexes were immobilized and counted on nCounter analyzer. Background subtraction was applied to raw data and samples were then normalized based on the geometric mean of positive controls and internal housekeeping genes (*GUSB*, *SP2*) using the nSolver software (version 2.5).

Mice

6-8 week-old C57BL/6AnCrI and BALB/cAnCrI female mice were purchased from Charles River Laboratories (L'Arbresle, France). OTI, OTII, IFN- γ ^{-/-}, and IFNAR^{-/-} transgenic mice were kindly provided by Dr. Perruche (INSERM UMR1098, Paris, France). All experimental studies were approved by the local ethics committee in accordance with the European Union's Directive 2010/63. Epithelial tumor TC1 cells transfected with HPV-16 E6 and E7-derived proteins and B16-F10 melanoma cells transfected or not with ovalbumin (B16-OVA) were kindly provided by Pr. Tartour (INSERM U970, Paris, France). CT26 and MC38 colon cancer cells were purchased from ATCC (CRL-2638 AND CRL-2839 respectively, ATCC American Type Culture Collection, Manassas, VA). All cell lines were cultured in RPMI 1640 medium supplemented with 10% fetal calf serum and 1% penicillin plus streptomycin (Gibco, France). Upon receipt, each cell line was expanded and stock vials were frozen. Each cell line was cultured no longer than one week after thawing a cryotube from the original stock.

Tumor rechallenge and T cell depletion experiments

For tumor re-challenge experiments, naïve and tumor-free mice were injected subcutaneously with 2.10^5 TC1/MC38 cells in the left flank and with 2.10^5 B16F10 or TC1 cells in the right flank. For CD4, CD8, IFN γ , and IFNAR1 T-cells depletion experiments, anti-mouse CD4⁺ (GK1.5, Euromedex), CD8⁺ (YTS 169.4, Euromedex), and IFNAR (MAR1-5A3, Euromedex) antibodies were used. CD8⁺ and CD4⁺ T-cell depletions started at day 7 post-CRT and mice were three times injected with 250 μ g of each antibody every 3-4 days. Injections with IFNAR blocking antibodies (five injections/200 μ g/mouse) started concurrently to CRT and were performed every 3 days.

TILs and RNA isolation

Briefly, tumor tissue dissociation was obtained by enzymatic digestion in GentleMACS Dissociator (Miltenyi Biotec) and lymphocytes were separated using Percoll gradient (Sigma Aldrich). Tumor cells were collected in the upper phase and TILs were recovered in the middle phase. For RNA sequencing experiments, TILs from 6 mice/treatment group were collected in RLT lysis buffer (Qiagen, France) and total mRNAs were extracted using the RNeasy Mini Kit according to the manufacturer's instructions (Qiagen, France). Extraction of ribosomal RNA (rRNA) from total RNA recovered was performed using the NEBNext rRNA depletion kit (New England BioLabs). Then, 100 ng of the RNA

mixture was used for preparation of sequencing libraries, which were sequenced on an Illumina NextSeq 500 device using paired-end 75-base pair reads.

Transcriptome analysis

Transcriptome analyses were performed using R software. Reads were mapped to the annotated mouse genome using the STAR splice aligner with the 2-pass protocol. Htseq-count script (version of May 2019) provided read counts per genes. Protein coding genes were selected. Genes presenting no expression (below 5 reads in total) were removed and the upper-quartile normalization method was applied. The correlation matrix over the eight experimental conditions was calculated for the most variable genes. Variance of the log₁₀ (fold change) expression was calculated for each tumor type after selecting genes presenting more than 50 reads in each experimental condition. We clustered genes by hierarchical clustering (clusters were defined on correlation coefficients matrix) using the Euclidian distance and Ward methods and generated using R package and Morpheus software (<https://software.broadinstitute.org/morpheus/>). Gene Set Enrichment Analysis (GSEA) in each cluster was performed using the full PanglaoDB database (version of May 2019). We used Benjamini and Hochberg corrected p-value of the hypergeometric test for further selection of cell types. Numbers of differentially expressed genes (DEGs; Log₂ fold change [FC] ≥ 3 or ≤ -3) regulated in TILs from each treatment group were measured using the Venny 2.1 software. Gene ontology analysis of the screened DEGs was carried out using the Metascape tool (<http://metascape.org>). Absolute abundance of immune cells in mouse tumors was quantified using the Microenvironment Cell Populations (MCP) counter R package. For each cell type, the abundance score was computed as the genomic mean expression of each mouse cell-type-specific gene [2].

Flow cytometry

To discriminate live from dead cells, samples were first stained with aqua Zombie viability dye (eBiosciences), then washed, stained with surface antibodies followed by the fixation and permeabilization of cell membrane by the Bioscience Fixation/Permeabilization kit (BD Biosciences). Following, samples were stained with intracellular antibodies according to the manufacturer's instructions. All antibodies used are referenced in the **Supplementary**

table S2. All stained samples were acquired by a BD FACSCantoII cytometer and analyzed using BD FACSDiva software (BD Biosciences).

Functional analysis of TILs

T cells activation state was monitored by intracellular staining of GzmB, Ki67, TNF α , and IFN- γ after overnight stimulation with R9F (HPV16E7₄₉₋₅₇), AH1 (gp70₄₂₃₋₄₃₁) (10 μ g/mL, JPT, Germany) derived-peptides, NA/LE purified CD3+/CD28+ antibodies (DB Biosciences), in the presence of GolgiPlug (1 μ l/mL) and GolgiStop (0.6 μ l/mL; BD Biosciences), according to the manufacturer's instructions. In some experiments, *ex vivo* IFN γ ELISpots assays were performed according to the manufacturer's instructions (Diaclone, France). Briefly, splenocytes, TILs were plated at 1.10⁵ cells/well and stimulated with tumor-derived peptides (R9F: HPV16E7₄₉₋₅₇), AH1 (gp70₄₂₃₋₄₃₁), A9M (ASMTNMELM) or PMA/ionomycine at 37°C for 15-20 hours. The IFN γ spot-forming cells were revealed following the manufacturer's instructions and counted using the C.T.L. Immunospot counter (Cellular Technology Ltd.).

Dendritic cells (DC) isolation and coculture with T-cells

For cross-presentation experiments, DCs from the tumor-draining lymph nodes of B16OVA tumor-bearing CRT-treated mice were sorted with magnetic microbeads conjugated with anti-CD11c antibodies (Miltenyi Biotech, France) and were pulsed for two hours with SL8 or OVA₃₂₃₋₃₃₉ peptides. After the incubation, DCs were washed for two times in PBS1X and cocultured with OTI and OTII cells that were previously recovered from the spleen of naïve OTI and OTII mice. Next, 9.10⁴ DCs were cultured in ELISpot plate with 1.10⁵ OTI or OTII T cells for 15-20 hours. T-cell reactivity was measured by the IFN- γ ELISpot assay as previously described.

Supplementary Table S2: List of antibodies

REAGENTS	SOURCE	IDENTIFIER
Mouse antibodies		
Percpcy5.5-anti CD3 (clone 145-2C11)	Biolegend	Cat# A94681
APCcy7-anti-CD4 (clone GK1.5)	Biolegend	Cat# 100414
Pacific Blue-anti-CD4 (clone GK1.5)	Biolegend	Cat# 1000428
APC/Fire 750-anti-CD4 (clone GK1.5)	Biolegend	Cat# 100460
APC-anti-CD8(clone53-6.7)	Biolegend	Cat# 207080
FITC-anti-CD8(clone53-6.7)	Biolegend	Cat# 140404
APC-anti-PDL1(cloneB7-H1)	Biolegend	Cat# 124312
PE-anti CD25 (clone PC61.5)	Biolegend	Cat# 102008
APC-anti IFNg (clone XMG1.1)	Biolegend	Cat# 505810
FITC-anti CD45 (clone 30-F11)	Biolegend	Cat# 103107
FITC-anti-CD103 (clone 2E7)	Biolegend	Cat# 121420
PE-anti TIM3 (clone B82C12)	Biolegend	Cat# 134014
Brillant violet421-anti TNFa (clone MP6-XT22)	Biolegend	Cat# 506328
PE-anti-CD44 (clone IM7)	Biolegend	Cat#103007
Pacific Blue-anti-CD62L (clone AEL14)	Biolegend	Cat# 104424
PE/Cy7-anti granzymeB (clone ICFC)	Biolegend	Cat# 372213
PE/Cy7-anti CD107 (clone 1D4B,BD)	BD Biosciences	Cat# 560647
APC-anti CD11b (clone M1/70)	eBiosciences	Cat# 17-0112-82
APC-anti Foxp3 (clone FJK-16s)	eBiosciences	Cat# 17-5773-82
FITC-anti Ki67 (clone SolA15)	eBiosciences	Cat# 11-5698-80
Anti-mouse PD1 (clone RMNP1-14)	Euromedex	Cat # BE0146
Anti-mouse PD-L1 (clone B7-H1)	Euromedex	Cat# BE0101
Anti-mouse CTLA4 (clone 9H10)	Euromedex	Cat# BE0131
Anti-mouse IFNAR1/2 (clone MAR1-5A3)	Euromedex	Cat# BE0241
Anti-mouse CD4 (clone GK1.5)	Euromedex	Cat# BE0003
Anti-mouse CD8 (clone YTS169.4)	Euromedex	Cat# BE0004
Vioblue-anti PD1 (clone HA2-7B1)	Miltenyi	Cat# 130-102-741
PEvio770-anti CD40 (REA602)	Miltenyi	Cat# 130-116-037
APC-anti CD80 (clone 1610A1)	Miltenyi	Cat# 130-102-584
Percpvio700-anti CD11c (REA754)	Miltenyi	Cat# 130-110-842
Vioblue- anti IA/IE (REA813)	Miltenyi	Cat# 130-112-237
APCVio770-anti CD8 (REA601)	Miltenyi	Cat# 130-120-806
PE-conjugatedE7 49-57 RAHYNIVTF Dextramers	Immudex	Cat# JA2195

- 1 Fehrenbacher L, Spira A, Ballinger M, *et al.* Atezolizumab versus docetaxel for patients with previously treated non-small-cell lung cancer (POPLAR): a multicentre, open-label, phase 2 randomised controlled trial. *Lancet* 2016;**387**:1837–46. doi:10.1016/S0140-6736(16)00587-0
- 2 Becht E, Giraldo NA, Lacroix L, *et al.* Estimating the population abundance of tissue-infiltrating immune and stromal cell populations using gene expression. *Genome Biol* 2016;**17**:218. doi:10.1186/s13059-016-1070-5